Tufts UNIVERSITY | School of Dental Medicine

Influence of zirconia crowns artifacts on cone beam computed tomography and image superimposition for digital planning and guided surgery

A Thesis

Presented to the Faculty of Tufts University School of Dental Medicine

in Partial Fulfillment of the Requirements for the Degree of

Master of Science in Dental Research

by

May Alaidrous

07 2019

THESIS COMMITTEE

Thesis Advisor

André B. de Souza, DDS, MSc

Assistant Professor

Department of Prosthodontics - Tufts University School of Dental Medicine

Committee Members

Matthew Finkelman, Ph.D.

Associate Professor

Department of Public Health and Community Service - Tufts University School of Dental Medicine

Yukio Kudara, C.D.T., M.D.T., R.D.T

Technical Instructor

Department of Prosthodontics - Tufts University School of Dental Medicine

Dr.Khaled El Rafie, DMD, FACP

Assistant Professor

Department of Prosthodontics - Tufts University School of Dental Medicine

Dr. Yongjeong Kim D.M.D., M.S., F.A.C.P.

Associate Professor

Associate Director of the Advanced Education Program in Prosthodontics

Department of Prosthodontics - Tufts University School of Dental Medicine

Dr Hugo C. Campos DDS, MDS, Diplomate ABOMR

Assistant professor

Oral and maxillofacial Radiology

Department of Diagnostic Sciences - Tufts University School of Dental Medicine

ABSTRACT

Aim & Hypothesis: The purpose of this in vitro study was to evaluate the effect of zirconia crowns restorations on the accuracy of superimposition process and guided surgery.

Materials & Methods: Four stone casts generated four groups: a control group (CG) with no crowns and three test groups with 4 (TG4), 7 (TG7) and 13 (TG13) zirconia crowns. A total of 40 cone beam computed tomography (CBCT) scans were taken for the four groups (10 CG, 10 4CG, 10 7CG, 10 13CG). All CBCTs were imported into the computer planning software (CoDiagnostiX, Dental Wings, Montreal, Canada) and the casts from all four groups were scanned with a high-resolution laboratory scanner. The obtained STL files were imported into the computer planning software. For each obtained DICOM dataset, segmentation was performed; superimposition of the three files was done for all the groups. The accuracy of superimposition was assessed, in millimeters, in three planes corresponding to anterior-posterior, horizontal and vertical planes.

Results: The overall analysis demonstrated significant differences between CG and TG7, CG and TG13, TG4 and TG7, TG4 and TG13, and TG7 and TG13 with $P<0.001$ for all of them. The anterior-posterior dimension demonstrated significant differences between CG and TG7 ($P<0.001$), CG and TG13 ($P<0.001$), TG4 and TG7 ($P=0.004$), and TG4 and TG13 ($P=0.001$). For the vertical dimension analysis, significant differences were found between CG and TG7 ($P<0.001$), CG and TG13 ($P<0.001$), TG4 and TG7 ($P=0.023$), and TG4 and TG13 ($p=0.005$). For the horizontal dimension, statistically significant differences between CG and TG7 ($p=0.049$), CG and TG13 ($p<0.001$), TG4 and TG13 ($p<0.001$), and TG7 and TG13 ($p=0.003$) were observed. There was no statistically significant difference between groups CG and TG4 ($p>0.05$). The highest discrepancy was observed in TG13 with average of 0.482 mm and the lowest discrepancy was found in the control group with average of 0.234 mm.

Conclusion: The accuracy of superimposition can be greatly influenced by the number of zirconia crowns artifacts in the CBCT image. This can reflect itself as 0.5 mm in horizontal and 1 mm in vertical directions. The higher the number of zirconia restorations, the lower the

accuracy of images' superimposition. Further research is needed to investigate the effect of different distribution of artifacts on image's superimposition accuracy.

ACKNOWLEDGMENTS

I woulk like to thank my personal instructor Dr.De Souza for his time, guidance and effort.

I would like to thank my committee members for their constant help and guidance.

Dr.Campos

Dr.Finkleman

Mr.Kudara

Dr.ELRafie

Dr.kim

I would like to thank Dr.Bahaa AlShawaf for his support and help in the study design.

TABLE OF CONTENTS

LIST OF TABLES

LIST OF FIGURES:

INFLUENCE OF ZIRCONIA CROWNS ARTIFACTS ON CONE BEAM COMPUTED TOMOGRAPHY AND IMAGE SUPERIMPOSITION FOR DIGITAL PLANNING AND GUIDED SURGERY

The use of digital technology is becoming a common practice in all different aspects of dentistry [1]. Computers can nowadays help the clinician diagnosing, treatment planning and executing the actual dental treatment. The introduction of digital technology in dentistry eliminated the space required for storing patients' records and files including x-rays, digital photographs and models. It also maintains the quality of records and facilitates records retrieval for future use. There are several new digital technologies that are being used in dentistry such as taking digital x-rays which allow instant assessment, completely eliminating the need for dark room and the maintenance of the fixating solution.

In the instance of taking digital impression of either natural dentition or implants, patients reported better comfort due to elimination of impression material [2]. Many other advantages are available with digital impressions including elimination of tray selection, reduced risk of distortion during impression making and pouring, disinfection, and shipping to the dental laboratory [3, 4]. Additionally, the digital scans can be communicated and stored electronically as digital information, improving efficiency and reducing costs.

The digital scan leads to a virtual cast that can generate a physical cast through milling or printing if a combination of digital and conventional workflow is needed [5]. Other advantages of digital impressions are the ability to edit, crop un-needed parts and the elimination of both bubbles and drags. Digital impressions can be stored for future use without the risk of dimensional changes as it is always a major disadvantage that we encounter with conventional impressions.

More advantages in the utilization of digital dental technology allowed faster execution of clinical and laboratory procedures [2]. It also enabled clinicians to maintain a specific level of acceptable standards regardless of their clinical experience [2]. Another important factor that made patients more in favor of digital technology in dentistry is the ability to manufacture crowns on the same day of teeth reparation by using chairside milling machines, hence the term same day restoration [6]. The development of high quality efficient intraoral scanners with comparable accuracy to conventional impression materials allowed clinicians to record the final impression data and produce the prosthesis in one day[6]. The time that is usually consumed in pouring the impression and the need for a laboratory to fabricate the restoration is eliminated

with this technology [6]. Clinicians are able to transfer the obtained data to design software, which provides a library of teeth morphology for final restoration design before sending it to a chair-side milling machine [6]. This process saves time, reduces procedure cost and eliminates additional lab fees, standardizing quality and reducing the impact of clinician experience. [6, 7] Hence, it reduced the gap existing between the quality of dental care provided by experienced and neonate practitioners. Furthermore, the actual clinical time to perform the procedure was less when digital technology was implemented [2]. This resulted in more patient satisfaction due to the time saved and the avoidance of using conventional impression material, which causes patient discomfort [2, 8].

One of the major advantages of digital technology is the advancement in dental implants planning and placement. This includes the digital tools for examination such as cone beam computed tomography (CBCT) prior to implant placement which was invented in the mid-nineties at a reasonable cost and low dose. It allows for a three dimensional view of the available volume of hard and soft tissue. It also contributed more to virtual planning of the surgical procedure and connecting both surgical and prosthetic plans together through implant planning software, it shows the proximity of the future implant to the patient's anatomical structures (maxillary sinus, inferior alveolar nerve, mental foramen and any pathologic lesions). This software is capable of generating a surgical guide design, which can be milled or printed to reduce the errors and complications generated by both the patient and the clinician, and limits the deviation of implant position during surgery.[9] This allows clinicians to achieve a prosthetically driven implant placement. [10]

The rise of this digital technology and its advantages made it a critical tool in improving the quality of implant prosthesis. The success of implant prosthesis starts from the detailed precise examination of patients' anatomy, ideal design of implant prosthesis and prosthetically driven implant placement.

The use of conventional x-rays in assessing alveolar bone defects was a common practice in dentistry [11]. However, it has a number of limitations, which affect the amount of information gained during the clinical examination. Conventional x-rays can give good information regarding the height of alveolar bone in the assessed area. However, it projects all

the information in a 2D view; thus the information regarding alveolar bone in buccal-lingual direction is missing [12]. Another limitation of 2D x-rays is the superimposition of anatomy and geometric distortion that makes the assessment of bone defect more challenging [13, 14]. Additionally, when using conventional 2D x-rays clinicians are not able to distinguish the buccal cortical plate from the lingual cortical plate that complicates assessing the existing bone defect [15].

In 1998 CBCT was introduced into dentistry especially for treatment planning implant surgeries and it offered many advantages over conventional 2D x-rays and CT scans [15]. CBCT enabled clinicians to visualize in 3D the anatomy of jaw with bone architecture, existing defects and vital structures [15]. The more details gained from CBCT regarding alveolar bone dimensions and existing bone defects improved the surgeons' understanding of the clinical situation with needed surgical procedures. The most valuable information obtained from the CBCT scan is highly accurate information on alveolar ridge width and height in addition to the bone density [15].

The implant placement surgical procedure can be very challenging because of the movement of the patient while drilling, local anesthetic wearing off causing limited surgery time, a limited visualization of the operation field and mental transfer of two-dimensional radiographs into the three-dimensional surgical site. As a consequence, implant malpositioning is associated with increased risk of damaging anatomical structures (e.g. maxillary sinus, mandibular canal) as well as an increased challenge to perform an appropriate final prosthesis. In addition, recent studies have shown that inappropriate implant position increases significantly the patients' risk to develop peri-implantitis [16].

Thus, surgical virtual planning and guided implant surgery have been considered an important tool for clinicians to assure appropriate three-dimensional implant positioning, especially in cases with complex anatomical structures and/or future prosthesis [17]. This technology involves the virtual implant placement, design and production of surgical guides using the CAD/CAM system. Recent developments have increased significantly the predictability of guided implant surgery [18]. The high predictability of guided surgery became

possible with the aid software that enables the superimposition of an STL file (three-dimensional intra-oral surface image) obtained from intra-oral scanner and the Digital Imaging and Communications in Medicine (DICOM) file from the CBCT. The superimposition of these files is crucial to obtain predictable outcomes in the guided surgery since the surgical guide rests on the STL file. Thus, any mismatching in the superimposition process will automatically be transferred to the implant position related to alveolar bone.

There are various types of conventional implant surgical guides that are used regularly to guide surgeons during the osteotomy and implant delivery. These guides allow a lot of freedom for the surgeon during the surgery to elect ideal position. This results in major complications and discrepancy in the final prosthesis if the surgeon was distracted and implants were placed in the wrong position. The use of digital technology in dentistry introduced virtual planning software that allows clinicians to connect the final prosthetic plane to the patient's anatomy in order to decide on the ideal implants position [7]. This position can be assessed virtually by merging implants to the CBCT and the future prosthetic dimensions in the virtual planning software. Digital technology allows the transfer of the planned implant position from the digital plane to the patient's mouth through printed or milled surgical guide that is generated and designed from that plane. These guides can limit the freedom of the surgeon in terms of osteotomy and implant 3D positioning. Hence, the outcome of complex cases can be more predictable and the complication of implant misplacement can be reduced [18].

Surgical guides can be used for partially edentulous and complete edentulous patients through the use of teeth-supported, mucosa or bone supported surgical guides. Indication of each type is self-explanatory, teeth supported surgical guides are indicated with bounded partially edentulous spaces. Whereas, mucosa or bone supported surgical guides are indicated for edentulous patients or with free end partially edentulous patient. In the case of bone supported guide a flap is reflected to allow the surgical guide to rest on the bone [19]. Recent studies have shown that teeth supported surgical guides are more accurate than mucosa or bone supported surgical guides; this conclusion was attributed to the resiliency of the mucosa that will cause slight movement of the surgical guide and to the inability to completely

eliminate the soft tissue from the DICOM file when designing bone supported surgical guides [20, 21].

Current literature classifies the complications of implant prosthesis into biological and technical categories [22]. Both complications are minimized by careful examination of patients and electing the ideal implant position depending on future teeth location and prosthesis design. Hence the term prosthetically driven implant placement evolved, which focused on placing the implants in ideal position to the final prosthesis rather than in the area of maximum bone.

Two common designs of implant prosthesis are available: screw- and cement-retained prosthesis [22]. The cement retained prosthesis design is more forgiving compared to the screw retained design in terms of planned and actual implant position. However, for both designs implants position should not deviate majorly from the planned position to achieve long-term successful prosthesis [23]. The screw-retained design is superior to cement retained design in terms of retrievability, which allows easy maintenance and repairs. Another major advantage of screw-retained prosthesis is the elimination of luting cement. It is currently known that excess luting cement in implant prosthesis is very difficult to remove. This can precipitate to implant failure and cause the development of peri-implantitis [22]. Screw-retained prosthesis can only be achieved by preplanning the implant positions depending on the prosthetic plan and precise placement of all implants in the ideal position and depth. This can be a very challenging procedure that is influenced by many factors such as patients' anatomy and surgeon's clinical skills. Other design factors that influence the success of implant prosthesis is avoiding the ridge lap design and distribution of implants in an edentulous arch. Identifying the correct implant position and placing the implants in complete edentulous cases is a very challenging procedure. This is mainly due to lack of all references from adjacent dentition and major changes in alveolar bone post exodontia. The ability to correctly distribute implants and place them in the correct 3D position is challenging even for experienced implant surgeons [24].

In fully edentulous patients, the ideal tooth position is visualized via a dual (or double) scan procedure, so that the virtual implants can be positioned by superimposing both

anatomical file to prosthesis file [25]. When dual scan technique is used, radio-opaque fiducial markers are attached to the prosthesis to be scanned. Two DICOM files will be obtained for the patient, the first with the prosthesis or teeth set-up is placed intra-orally. The second scan is to be taken of the prosthesis at different exposure parameters. This will allow the visualization of future teeth position and its superimposition to hard and soft tissue anatomy [25].

In partially edentulous patients the STL files are obtained either intraorally using intraoral scanners or extra-orally through desktop scanner, scanning an accurate model of the existing intra-oral condition. To obtain an STL file of planned prosthesis either an intraoral scanner is used to scan the existing provisional or extra-orally through scanning wax up using lab scanner or through using software wax-up library. The process of images' superimposition and data registration requires importing a DICOM file (patient's CBCT) to at least one STL file into digital implant planning software. Data registration consists of several steps starting with segmentation (three-dimensional image reconstruction from CBCT), orienting the image in relation to different planes, tracking anatomical structure such as the inferior alveolar nerve (IAN) and merging of the file together. The process of CBCT image segmentation, the elimination of undesirable anatomical information and distortion, such as scatter from metal artifacts allows a better view of the area of interest using the gray-value threshold. The obtained refined files are supper imposed by selecting corresponding teeth and identical fiducial landmarks that allow merging of the two files. This step allows for the clear view of the bone volume, virtual implant planning and the future prosthesis design [26]. There are several factors that could potentially affect the accuracy of static guided implant surgery such as the patient, operator and data acquisition. These factors are described below individually.

Flapless and flap guided surgery

Flapless surgery is defined as the insertion of an implant through the trans-mucosal tissue without reflecting the mucosa. The advantage of this technique is to maintain the blood supply around periosteum, hence, reduce the amount of bone loss, it also helps the papilla to regrow and develop [18]. Guided implant surgery is considered the tool for that as it saves the

time required for flap elevation and suturing.

Surgical guide-related factors

There are different types of surgical guides, bone-mucosa supported or teeth-supported. The difference in inaccuracy between the two types was clinically insignificant, but studies show that teeth-supported surgical guides are more accurate [27].

Software-related factors

There are different implant planning software systems in the market; some allow for fully guided implant planning and some allow for partially guided implant planning. Fully guided implant surgery seems to be more accurate and consistent in comparison with partially guided or conventional surgery. The accuracy between fully guided implant planning software systems depends mainly on the ability of the software to register the fiducial referential markers (gutta-percha or spherical radiopaque markers) on CBCT and/or the ability to accurately align it well to the teeth surface with tomographic image, in other words, superimpose the files obtained from CBCT (DICOM) to the scans (STL).[21]

Patient-related factors

There are several factors related to patients that can potentially affect the accuracy of static guided implant surgery. Movement of the head of the patient during taking the CBCT can greatly influence the quality of the image. Although head fixating devices are present, it still allows for some degree of motion. Pettersson *et al.* showed that there was a significant difference in the position of the planned implant compared the final implant position in the apex and platform area. Patients' tolerance to surgical instruments and devices intra-orally also can affect implant placement. Particularly in posterior sites, there is frequently limited mouth opening space for handles, hand piece and guided drills. [21]

Operator's experience-related factors

It has been claimed that experience is not a primary prerequisite for guided implant

surgery and the lack of operator's experience will not affect the accuracy of guided surgery. However, studies by Hinckfuss in 2012 showed that the amount of discrepancy is increased with novice and intermediate dentists compared to well-trained dentists. [28]

Imaging related factors:

CBCTs have common types of artifacts that could limit the image quality, such as motion artifact, beam hardening and metal scatter. Inherent artifact in CBCT imaging that is related to the movement of the head of the patient are limited by certain algorithm. This algorithm is specific to each CBCT machine to rectify these errors, up to date studies indicate that these errors are not fully eliminated [29, 30]. Several ways have been introduced to minimize the movement of the patient's head. Example of these techniques are using the bite tap, cotton rolls or instruct the patient to close their eye and prevent tracking the x-ray head as it rotates. Beam hardening is manifested as the dark line around the high-density restorations, due to the border between the sudden difference in density between the very dense restoration and the not so dense tooth structure.

Metal artifacts are manifested as the horizontal star shaped pattern of x-ray images that are present around dense restorations such as amalgam, gold and PFM restorations. CBCT and all other types of x-rays are registered by energetic XRAY photons. Setting the kVp (peak kilo-voltage) to a certain number for example 70 means that the strike beam energy is 70 kVp and the average beam energy is approximately 30-20 kVp. When the primary beam strikes around dense metal restorations, these dense metal restorations tend to reduce or weaken the lower energy. As a result of this the detector can only register the highest energy photons [31, 32].

The most used landmark for images' superimposition in digital planning and guided surgery in dentate patients is teeth . Once they are clearly visible on the STL file and on the three-dimensional reconstruction (e.g segmentation) from the CBCT [31]. Therefore, the step of superimposition is more challenging when patients present with metal restorations due to the presence of artifacts from the CBCT, which might affect the accuracy of superimposing images using the anatomical landmarks. Particularly, restorations made of zirconium that became very popular in the past years present high radiopacity. Artifacts produced from this type of

restoration can potentially influence the quality of three-dimensional reconstruction from the CBCT. It is noteworthy that even though guided surgery has become a more common procedure, there is a lack of evidence in the literature regarding the effect of the artifacts in the images' superimposition process for guided implant surgery [31, 32].

AIM AND HYPOTHESIS

The aim of this in vitro study was to evaluate the effect of zirconia crowns restorations on the accuracy of superimposition process for guided implant surgery. The hypothesis was that there is an increased discrepancy in superimposition for guided implant surgery with the increase of zirconia crowns numbers.

SIGNIFICANCE

Guided implant surgery has become a very common practice by dentists from all over the world. However, there is still a lack of information in the literature regarding whether the amount of restorations could potentially decrease the predictability of images' superimposition and consequently, implant placement. By knowing the effect of artifacts in the superimposition process we are able to make an accurate prediction of guided surgery in patients with restoration. This research forms a basis for determining the number of zirconia crowns that could potentially decrease the predictability of guided surgery.

MATERIALS AND METHODS

A dentate mandible with missing tooth #20 was printed from Standard tessellation language (STL) datasets using 3D Stereolithography (SLA) printer (Vareso, BEGO). Four rectangular markers were attached to the printed mandibular cast at 10mm apical to the buccal

gingival (Figure 1). The printed cast was duplicated with silicone material (Z-Dupe, Henry Schein Inc) and then poured with type IV stone (Resin Rock, Wipmix). Four stone casts were generated from the duplication material and thereby generated four groups (Figures 2 and 3); each group was comprised of 1 master cast, 10 CBCTs (DICOM files) and 1 (STL files). The studied groups were as following:

1- Control group (CG): the stone master cast received zero zirconia crowns and was designated as the control group.
2- Test Group 4 (TG4): the stone master cast received four zirconia crowns on first molars and first premolars.
3- Test Group 7 (TG7): The stone master cast received seven zirconia crowns on all molars and premolars except #20.
4- Test Group 13 (TG13): the stone master cast received 13 zirconia crowns on all teeth from second molar to second molar except #20.

Zirconia Crowns Fabrication

Teeth that received zirconia crowns in all groups were prepared by the primary investigator with 1.5mm reduction axially and 2mm reduction occlusally. A coarse diamond chamfer bur (ISO 18 Brasseler, USA) was used for the reduction and fine diamond bur (ISO 18, Brasseler, USA) was used to smoothen the abutment preparations. The established margin was 1mm supragingival deep chamfer and all preparation line angles were rounded. The teeth preparations were scanned with high accuracy laboratory scanner (calibrated according to the manufacturer's instructions) (Activity 880scanner, Smart Optics, Bochum, Germany) and the STL files were imported into designing software to complete the design (Exocad GmbH, Germany). Full contour zirconia crowns (Katana, Kuraray Noritake Dental Inc.) were milled with a 5 axis milling machine that was calibrated according to the manufacturer's instructions (Schutz Tizian cut 5®, Germany). The milled zirconia crowns were sintered using HT speed sintering furnace (Mihm-vogt, Blankenloch, Germany) that was calibrated according to the manufacturer's instructions at 1500° F for 2 hours holding with a total time of 13 hours. The crowns were

adjusted and fitted on the dies. All steps of crowns production were performed by a single dental technician.

CBCT Image

A total of 40 CBCT scans were taken for the four groups (10 CG, 10 4CG, 10 7CG, 10 13CG). All images were obtained from the same tomographic machine (i-CAT®, Imaging Sciences International, Inc., Hatfield, PA, USA) and taken by a single radiologist. All CBCTs were imported from MiPACs through export option into the computer planning software (CoDiagnostiX, Dental Wings, Montreal, Canada) as digital imaging and communication in medicine (DICOM) datasets.

Cast Scanner

All of the casts from all four groups were scanned with a high-resolution laboratory scanner (Activity 880scanner, Smart Optics, Bochum, Germany). The obtained STL files were imported into the computer planning software (coDiagnostiX, Dental Wings, Montreal, Canada). A total of 4 STL files were obtained and superimposed with the corresponding CBCT (Figure 4).

Images' Segmentation and Superimposition

Each obtained DICOM dataset was imported to the computer planning software (coDiagnostiX, Dental Wings, Montreal, Canada) and image segmentation was performed using the 3D reconstruction software feature. Before the segmentation process each 3D image was aligned at sagittal, coronal and axial views using defined criteria. Since the segmentation of the tomographic image is arbitrary, the density of gray values (HU) was established based on an initial superimposition of the fiducial markers with the scanned image (STL file). The fiducial markers were erased from the 3D reconstruction in order to reduce bias at the superimposition.

An experienced operator performed all of the segmentations and superimpositions. Each 3D image (DICOM) reconstructed was superimposed to the same DICOM file first to get a definite line that was used to measure the discrepancy and then was superimposed to its corresponding STL file taking four to six areas on the teeth surface, with at least two landmarks in the anterior and two in the posterior area (Figure 4).

Accuracy Evaluation

The accuracy of superimposition was assessed, in millimeters, by comparing the discrepancy between the fiducial markers. The distances from the CBCT image to the cast STL were obtained and measured using an open source software (Image J, National Institute of Health, USA) in three planes corresponding to anterior-posterior, horizontal and vertical planes (Figure 4).

Sample Size

A sample size calculation was conducted using the software nQuery Advisor (Version 7.0). Using the results of a pilot study for the expected within-group means and within-group standard deviation, a sample size of n = 10 per group was found to be sufficient to achieve greater than 99% power alongside a Type I error rate of 0.05.

Statistical Analysis

Descriptive statistics (means, medians, standard deviations, inter-quartile ranges, minima, and maxima) were calculated by group. Comparisons between the groups were conducted via one-way ANOVA, Welch's F test, or the Kruskal-Wallis test (with post-hoc testing conducted via Tukey's HSD, the Games-Howell test, or Dunn's test with the Bonferroni correction, respectively) depending on the validity of the statistical assumptions. The Shapiro-Wilk test was used to assess the assumption of normality, and Levene's test was used to assess the assumption of homogeneity of variances. The level of significance was established at $\alpha = 0.05$, with the exception of tests in which the Bonferroni correction was used. A separate

analysis was performed for each dimension (anterior-posterior, horizontal, and vertical), as well as for an overall measure of discrepancy in which the results of the three dimensions were averaged. SPSS version 25 was used in the analysis.

RESULTS

Significant non-normality was observed for the anterior-posterior and vertical variables. Therefore, the Kruskal-Wallis test (with Dunn's test with Bonferroni correction in post-hoc testing) was used for the anterior-posterior and vertical dimensions. For the horizontal dimension, neither significant non-normality nor significant evidence of violation of homogeneity of variance was observed ($P>0.05$). Hence, one-way ANOVA (with Tukey's HSD in post-hoc testing) was used for the horizontal dimension. For the overall analysis measure no significant non-normality was observed but significant evidence of violation of homogeneity of variances was found ($P<0.05$). Therefore, significance testing was conducted using Welch's F test and the Games-Howell test in post-hoc testing.

Descriptive statistics for the anterior-posterior dimension are shown in Table 1. The highest mean and median values were found in TG13, followed by TG7, TG4 and then the CG. The Kruskal-Wallis test was statistically significant ($P<0.001$). In post-hoc comparisons (Dunn's test with Bonferroni correction), significant differences were found between CG and TG7 ($P<0.001$), CG and TG13 ($P<0.001$), TG4 and TG7 ($P=0.004$) and TG4 and TG13 ($P=0.001$). Side-by-side boxplots are shown in Figure 5.

For the vertical dimension analysis, descriptive statistics are shown in Table 2. The least values for mean and median were shown in the control group, followed by TG4, TG7 and then TG13. The Kruskal-Wallis test was statistically significant ($P<0.001$). In post-hoc comparisons (Dunn's test with Bonferroni correction), significant differences were found between CG and TG7 ($P=0.001$), CG and TG13 ($P<0.001$), and TG4 and TG13 ($P<0.001$). Side-by-side boxplots are shown in Figure 6.

For the horizontal dimension, the one-way ANOVA test was statistically significant (P<0.001). In post-hoc comparisons (Tukey's HSD), there were statistically significant differences between groups CG and TG7 (P=0.049), CG and TG13 (P<0.001), TG4 and TG13 (P<0.001), and TG7 and TG13 (P=0.003). The highest discrepancy was observed in group TG13, and the lowest discrepancy was found in group CG (Table 3). Side-by-side boxplots are shown in Figure 7.

For the overall analysis, Welch's F test was statistically significant (P<0.001). In post-hoc comparisons (Games-Howell test), significant differences were observed between groups CG and TG7 (P<0.001), CG and TG13 (P<0.001), TG4 and TG7 (P<0.001), TG4 and TG13 (P<0.001), and TG7 and TG13 (P=0.006). The highest discrepancy was observed in group TG13, and the lowest discrepancy was found in group CG (Table 4). Side-by-side boxplots are shown in Figure 8.

DISCUSSION

Inaccuracies between the guided implant placement and the virtual implant planning was found to be clinically insignificant if 2 mm of safety margin was used, the discrepancy is accumulative and is carried out through the whole procedure starting with collecting the record, planning the implant position and the execution of the actual surgery [26].

Accurate superimposition of STL file to DICOM data is a critical step for controlled implant treatment planning in guided surgery. The accuracy of superposition is dependent on the quality of data obtained through the planning phase. In this study, artifacts from zirconia crowns on teeth were shown to be a major factor in reducing the quality of DICOM data sets by eliminating the details of the adjacent dentition in DICOM data set. The effect of scatter on superimposition accuracy was not significant in the group of four zirconia crowns due to the existence of enough details from non-crowned teeth. By increasing the number of crowns to seven, more artifacts were observed and less details present in non-crowned teeth. This reflected itself as noticeable discrepancy in all planes. By crowning all teeth in the thirteen

crowns group, all details were eliminated and discrepancy was maximized. The discrepancy was noticed more in the vertical dimension due to lack of any details to identify the level of superimposition in this plane. In other planes the structures below scatter level might have aided the software in positioning the STL file.

Zirconia is becoming more popular in dental practice due to its ability to be implemented in the digital workflow, as it is an inexpensive material. Therefore, for these reasons zirconia was the material of choice for this study**.** In a study comparing the amount of scatter caused by Zirconium dioxide, titanium and titanium–zirconium, the author found that the amount of artifacts depends on the type of material used. The artifacts generated by zirconium dioxide implants were significantly higher than artifacts produced by titanium and titanium–zirconium implants. The average artifacts intensity produced by zirconium dioxide implants was about threefold the artifacts produced by titanium implants [29, 33].

A study by Flugge et al. reported similar results with the discordance between CBCT and surface scan model occurring due to inaccurate registration or superimposition. This discrepancy is transferred to the surgical field and resulted in a significant discrepancy between the digital planned implant position and actual achieved implant position. The quality of imported data can have detrimental effect on the accuracy of digital implant planning in the software. Two factors were identified as possible source of error, the number of restorations present and the user. Eventually, both will result in clinically unacceptable drilling guides [33]. The use of anatomical landmarks for the superimposition of data in digital implant planning is advantageous as it reduces both the time taken and the number of appointments for the patient. Also the CBCT machine can have significant effect on the image quality produced for digital guided implant planning. In a study conducted to compare the I-CAT machine to the MSCT (multislice computed tomography) using HU (Hounsfield unit) in terms of bone density, results showed significant difference. The HU values were higher on CBCT than those obtained from MSCT which is considered the gold standard [34]. Another study conducted comparing grey values for bone density between CBCT and MSCT demonstrated that there is a large error when using the grey value in a quantitative way, although the CBCT and CT showed great

correlation in terms of their numbers [35]. In general, the amount of metal artifacts found in the CBCT can greatly influence the image quality and currently there is no effective method for eliminating the scatter around metal in CBCTs [7]. In another recent study, metal artifact reduction methods on filter based dual-energy CBCT were proposed using two techniques, alternative spectral switching and simultaneous beam splitting. It was concluded that pseudo-switching the metal filters between the x ray tube with upstream placement has a great effect in reducing metal artifacts [36]. This technique in taking the CBCT data might be helpful when placing implants in patients with full mouth metal restorations.

Another technique was developed using an algorithm in data processing to reduce the metal artifact in CBCT images. They used three components and tested the outcome of different technique combination. The first component used modeling of image histogram to extract teeth. The second one reduced artifacts by striking artifact reduction component through converting image into the polar domain and applying morphological filtering. The third component utilized morphological filtering operation to fill the cavities. The combination of the three processing techniques produced a clearer image and greatly reduced the artifacts [37].

In a recent in-vitro study comparing the accuracy between pilot drills guided and fully guided single implant placement, the authors found that there is a statistically significant higher accuracy with the fully guided approach in comparison with the pilot drill approach. Although the superimposition was accurate in terms of lack of metal scatter in the CBCT, the amount of discrepancy was statistically significant in the pilot-drill guided implant placement approach [38]. In another in vivo study that was conducted in 2019, the authors found that the use of static computer assisted implant surgery resulted in more accurate implant position when compared to freehand surgery in a single tooth edentulous space [39]. In a study comparing dynamic guided implant surgery to freehand implant placement, both placements presented comparable results [40]. However, dynamic navigation system is advantageous in regards to the ability of the surgeon to change and modify the implant position in relation to the prosthesis on the surgical site [41]. Therefore, in case of significant amount of metal restorations this system might be considered.

CONCLUSION

The accuracy of superimposition can be greatly influenced by the number of zirconia crowns artifacts in the CBCT image. This can reflect itself as 0.5mm in horizontal and 1mm in vertical directions. The higher the number of zirconia restorations, the lower the accuracy of images' superimposition. Further research is needed to investigate the effect of different distribution of artifacts on images' superimposition accuracy.

REFERENCES

1. Strub, J.R., E.D. Rekow, and S. Witkowski, *Computer-aided design and fabrication of dental restorations: current systems and future possibilities.* J Am Dent Assoc, 2006. **137**(9): p. 1289-96.
2. Lee, S.J. and G.O. Gallucci, *Digital vs. conventional implant impressions: efficiency outcomes.* Clin Oral Implants Res, 2013. **24**(1): p. 111-5.
3. Gimenez, B., et al., *Accuracy of a digital impression system based on parallel confocal laser technology for implants with consideration of operator experience and implant angulation and depth.* Int J Oral Maxillofac Implants, 2014. **29**(4): p. 853-62.
4. Gimenez, B., et al., *Accuracy of a Digital Impression System Based on Active Triangulation Technology With Blue Light for Implants: Effect of Clinically Relevant Parameters.* Implant Dent, 2015. **24**(5): p. 498-504.
5. Marghalani, A., et al., *Digital versus conventional implant impressions for partially edentulous arches: An evaluation of accuracy.* J Prosthet Dent, 2018. **119**(4): p. 574-579.
6. Blatz, M.B. and J. Conejo, *The Current State of Chairside Digital Dentistry and Materials.* Dent Clin North Am, 2019. **63**(2): p. 175-197.
7. Hammerle, C.H., et al., *Digital technologies to support planning, treatment, and fabrication processes and outcome assessments in implant dentistry. Summary and consensus statements. The 4th EAO consensus conference 2015.* Clin Oral Implants Res, 2015. **26 Suppl 11**: p. 97-101.
8. Yuzbasioglu, E., et al., *Comparison of digital and conventional impression techniques: evaluation of patients' perception, treatment comfort, effectiveness and clinical outcomes.* BMC Oral Health, 2014. **14**: p. 10.
9. Cassetta, M. and M. Bellardini, *How much does experience in guided implant surgery play a role in accuracy? A randomized controlled pilot study.* Int J Oral Maxillofac Surg, 2017. **46**(7): p. 922-930.
10. Vercruyssen, M., et al., *Guided surgery: accuracy and efficacy.* Periodontol 2000, 2014. **66**(1): p. 228-46.
11. Mengel, R., B. Kruse, and L. Flores-de-Jacoby, *Digital volume tomography in the diagnosis of peri-implant defects: an in vitro study on native pig mandibles.* J Periodontol, 2006. **77**(7): p. 1234-41.
12. Jervoe-Storm, P.M., et al., *Comparison of cone-beam computerized tomography and intraoral radiographs for determination of the periodontal ligament in a variable phantom.* Oral Surg Oral Med Oral Pathol Oral Radiol Endod, 2010. **109**(2): p. e95-101.
13. Patel, S., et al., *Detection of periapical bone defects in human jaws using cone beam computed tomography and intraoral radiography.* Int Endod J, 2009. **42**(6): p. 507-15.
14. Tyndall, D.A. and S.L. Brooks, *Selection criteria for dental implant site imaging: a position paper of the American Academy of Oral and Maxillofacial radiology.* Oral Surg Oral Med Oral Pathol Oral Radiol Endod, 2000. **89**(5): p. 630-7.
15. Ritter, L., et al., *Accuracy of peri-implant bone evaluation using cone beam CT, digital intra-oral radiographs and histology.* Dentomaxillofac Radiol, 2014. **43**(6): p. 20130088.
16. Canullo, L., et al., *Distinguishing predictive profiles for patient-based risk assessment and diagnostics of plaque induced, surgically and prosthetically triggered peri-implantitis.* Clin Oral Implants Res, 2016. **27**(10): p. 1243-1250.
17. Vermeulen, J., *The Accuracy of Implant Placement by Experienced Surgeons: Guided vs Freehand Approach in a Simulated Plastic Model.* Int J Oral Maxillofac Implants, 2017. **32**(3): p. 617-624.
18. D'Haese, J., et al., *Current state of the art of computer-guided implant surgery.* Periodontol 2000, 2017. **73**(1): p. 121-133.
19. Pettersson, A., et al., *Accuracy of virtually planned and template guided implant surgery on edentate patients.* Clin Implant Dent Relat Res, 2012. **14**(4): p. 527-37.
20. Ozan, O., et al., *Clinical accuracy of 3 different types of computed tomography-derived stereolithographic surgical guides in implant placement.* J Oral Maxillofac Surg, 2009. **67**(2): p. 394-401.
21. Pettersson, A., et al., *Accuracy of CAD/CAM-guided surgical template implant surgery on human cadavers: Part I.* J Prosthet Dent, 2010. **103**(6): p. 334-42.
22. Papaspyridakos, P., et al., *Complications and survival rates of 55 metal-ceramic implant-supported fixed complete-arch prostheses: A cohort study with mean 5-year follow-up.* J Prosthet Dent, 2019.
23. Wittneben, J.G., et al., *Screw retained vs. cement retained implant-supported fixed dental prosthesis.* Periodontol 2000, 2017. **73**(1): p. 141-151.

24. Choi, W., et al., *Freehand Versus Guided Surgery: Factors Influencing Accuracy of Dental Implant Placement.* Implant Dent, 2017. **26**(4): p. 500-509.
25. Vercruyssen, M., et al., *Computer-supported implant planning and guided surgery: a narrative review.* Clin Oral Implants Res, 2015. **26 Suppl 11**: p. 69-76.
26. Al Yafi, F., B. Camenisch, and M. Al-Sabbagh, *Is Digital Guided Implant Surgery Accurate and Reliable?* Dent Clin North Am, 2019. **63**(3): p. 381-397.
27. Van Assche, N., et al., *Accuracy of computer-aided implant placement.* Clin Oral Implants Res, 2012. **23 Suppl 6**: p. 112-23.
28. Hinckfuss, S., et al., *Effect of surgical guide design and surgeon's experience on the accuracy of implant placement.* J Oral Implantol, 2012. **38**(4): p. 311-23.
29. Benic, G.I., et al., *In vitro assessment of artifacts induced by titanium dental implants in cone beam computed tomography.* Clin Oral Implants Res, 2013. **24**(4): p. 378-83.
30. Sancho-Puchades, M., C.H. Hammerle, and G.I. Benic, *In vitro assessment of artifacts induced by titanium, titanium-zirconium and zirconium dioxide implants in cone-beam computed tomography.* Clin Oral Implants Res, 2015. **26**(10): p. 1222-8.
31. Fokas, G., et al., *Accuracy of linear measurements on CBCT images related to presurgical implant treatment planning: A systematic review.* Clin Oral Implants Res, 2018. **29 Suppl 16**: p. 393-415.
32. Wismeijer, D., et al., *Group 5 ITI Consensus Report: Digital technologies.* Clin Oral Implants Res, 2018. **29 Suppl 16**: p. 436-442.
33. Pjetursson, B.E., et al., *A systematic review of the survival and complication rates of zirconia-ceramic and metal-ceramic single crowns.* Clin Oral Implants Res, 2018. **29 Suppl 16**: p. 199-214.
34. Silva, I.M., et al., *Bone density: comparative evaluation of Hounsfield units in multislice and cone-beam computed tomography.* Braz Oral Res, 2012. **26**(6): p. 550-6.
35. Pauwels, R., et al., *Variability of dental cone beam CT grey values for density estimations.* Br J Radiol, 2013. **86**(1021): p. 20120135.
36. Iramina, H., et al., *Metal artifact reduction by filter-based dual-energy cone-beam computed tomography on a bench-top micro-CBCT system: concept and demonstration.* J Radiat Res, 2018. **59**(4): p. 511-520.
37. Johari, M., et al., *Metal Artifact Suppression in Dental Cone Beam Computed Tomography Images Using Image Processing Techniques.* J Med Signals Sens, 2018. **8**(1): p. 12-24.
38. Schulz, M.C., et al., *Pilot-drill guided vs. full-guided implant insertion in artificial mandibles-a prospective laboratory study in fifth-year dental students.* Int J Implant Dent, 2019. **5**(1): p. 23.
39. Smitkarn, P., et al., *The accuracy of single-tooth implants placed using fully digital-guided surgery and freehand implant surgery.* J Clin Periodontol, 2019.
40. Block, M.S., et al., *Implant Placement Accuracy Using Dynamic Navigation.* Int J Oral Maxillofac Implants, 2017. **32**(1): p. 92-99.
41. Block, M.S., et al., *Implant Placement Is More Accurate Using Dynamic Navigation.* J Oral Maxillofac Surg, 2017. **75**(7): p. 1377-1386.

APPENDICES

APPENDIX A: TABLES

Table 1: Mean, median, standard deviation (SD), interquartile range (IQR) and minimum to maximum (Min-Max) anterior-posterior values, in millimeters, between the different studied groups.

Groups	Mean	Median	SD	IQR	Min-Max	P value*
CG	0.197	0.213	0.065	0.153-0.225	0.096-0.325	<0.001
TG4	0.256	0.239	0.084	0.205-0.281	0.172-0.456	
TG7	0.480	0.472	0.093	0.402-0.572	0.340-0.602	
TG13	0.578	0.510	0.203	0.429-0.785	0.350-0.937	

*P-value based on the Kruskal-Wallis test. In post-hoc testing (Dunn's test with Bonferroni correction), significant differences were observed between groups CG and TG7, TG0 and TG13, TG4 and TG7 and TG4 and TG13.

Table 2: Mean, median, standard deviation (SD), interquartile range (IQR) and minimum to maximum (Min-Max) vertical values, in millimeters, between the different studied groups.

Groups	Mean	Median	SD	IQR	Min-Max	P value*
CG	0.204	0.178	0.112	0.120-0.241	0.089-0.470	<0.001
TG4	0.263	0.238	0.078	0.218-0.340	0.145-0.398	
TG7	0.560	0.548	0.129	0.446-0.668	0.367-0.752	
TG13	0.880	0.805	0.204	0.763-1.085	0.536-1.198	

*P-value based on the Kruskal-Wallis test. In post-hoc testing (Dunn's test with Bonferroni correction), significant differences were observed between groups CG and TG7, CG and TG13, and TG4 and TG13.

Table 3: Mean, median, standard deviation (SD), interquartile range (IQR) and minimum to maximum (Min-Max) horizontal values, in millimeters, between the different studied groups.

Groups	Mean	Median	SD	IQR	Min-Max	P value*
CG	0.234	0.247	0.066	0.162-0.296	0.152-0.318	<0.001
TG4	0.253	0.256	0.067	0.195-0.306	0.165-0.375	
TG7	0.338	0.351	0.073	0.292-0.391	0.191-0.443	
TG13	0.482	0.480	0.125	0.372-0.616	0.313-0.672	

*P-value based on one-way ANOVA. In post-hoc testing with Tukey's HSD, significant differences were observed between groups CG and TG7, CG and TG13, TG4 and TG13, and TG7 and TG13.

Table 4: Mean, median, standard deviation (SD), interquartile range (IQR) and minimum to maximum (Min-Max) of overall values, in millimeters, between the different studied groups.

Groups	Mean	Median	SD	IQR	Min-Max	P value*
CG	0.212	0.200	0.065	0.154-0.254	0.143-0.326	<0.001
TG4	0.258	0.252	0.059	0.217-0.283	0.173-0.388	
TG7	0.460	0.467	0.054	0.405-0.497	0.378-0.543	
TG13	0.646	0.619	0.131	0.529-0.743	0.491-0.919	

*P-value based on Welch's F test. In post-hoc testing with the Games-Howell test, significant differences were observed between groups CG and TG7, CG and TG13,TG4 andTG 7, TG4 and TG13, and TG7 and TG13.

APPENDIX B: FIGURES

Figure 1: (a) Printed mandible with attached four rectangular markers and (b) duplicated mandible in stone.

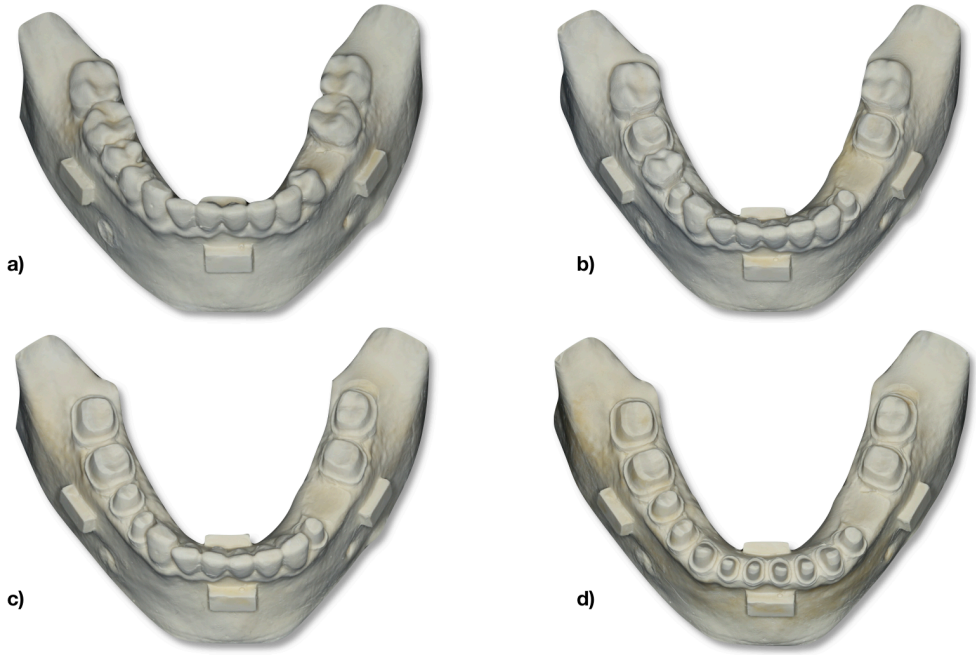

Figure 2: (a) Stone cast of control group (CG), (b) master cast of test four crowns group (TG4), (c) master cast of test seven crowns group (TG7), (d) master cast of test thirteen crowns group (TG13).

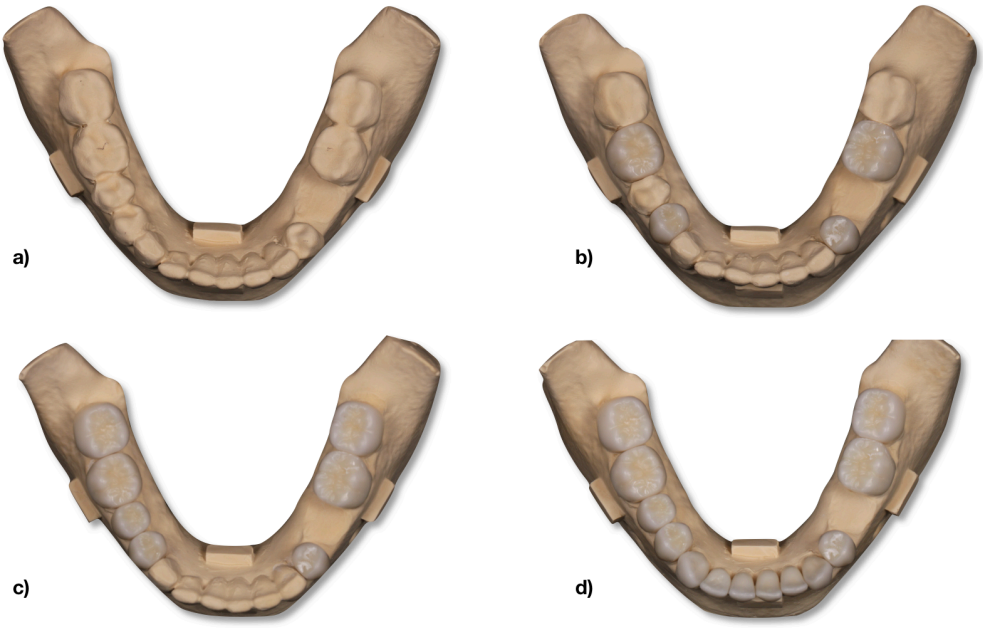

Figure 3: (a) Stone cast of control group (CG), (b) master cast with four zirconia crowns (TG4), (c) master cast with seven zirconia crowns (TG7) and (d) master cast with thirteen zirconia crowns (TG13).

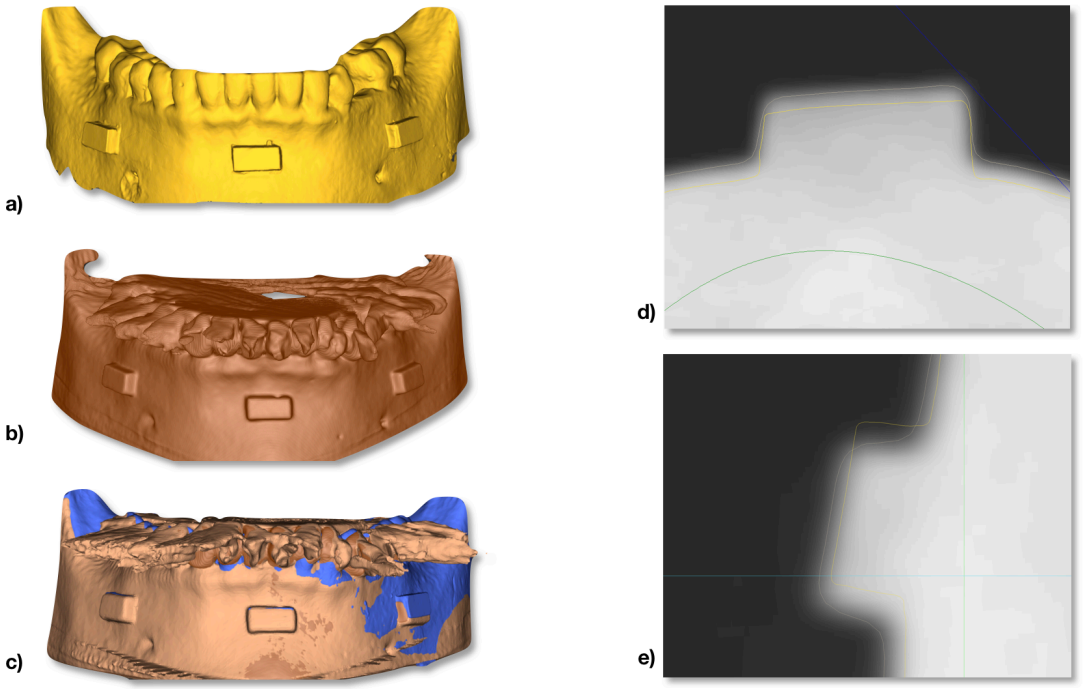

Figure 4: (a) STL file of the scanned TG13 model, (b) 3D construction of the CBCT (DICOM) file of TG13, (c) superimposition of STL & DICOM files, (d) screen shot of the slice to measure discrepancy in anterior-poster and horizontal planes using image-j software and (e) screen shot of the slice to measure discrepancy in vertical plane using image-j software.

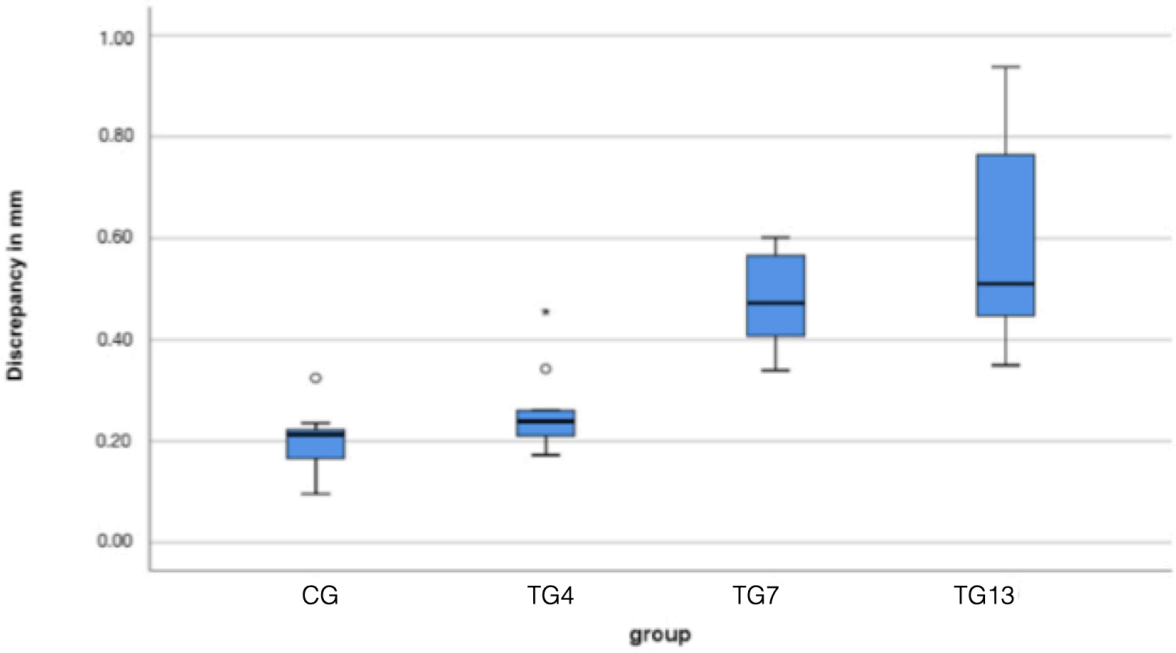

Figure 5: Side-by-side boxplots of the four groups, showing discrepancy in the anterior-posterior plane in millimeters.

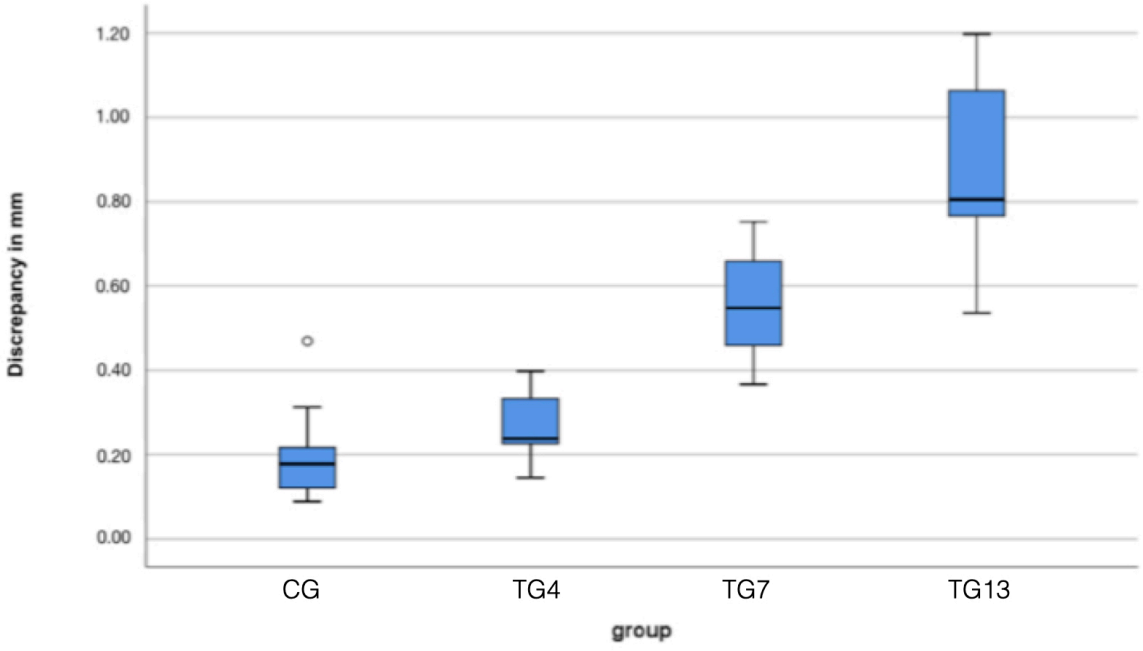

Figure 6: Side-by-side boxplots of the four groups, showing discrepancy in the vertical plane in millimeters.

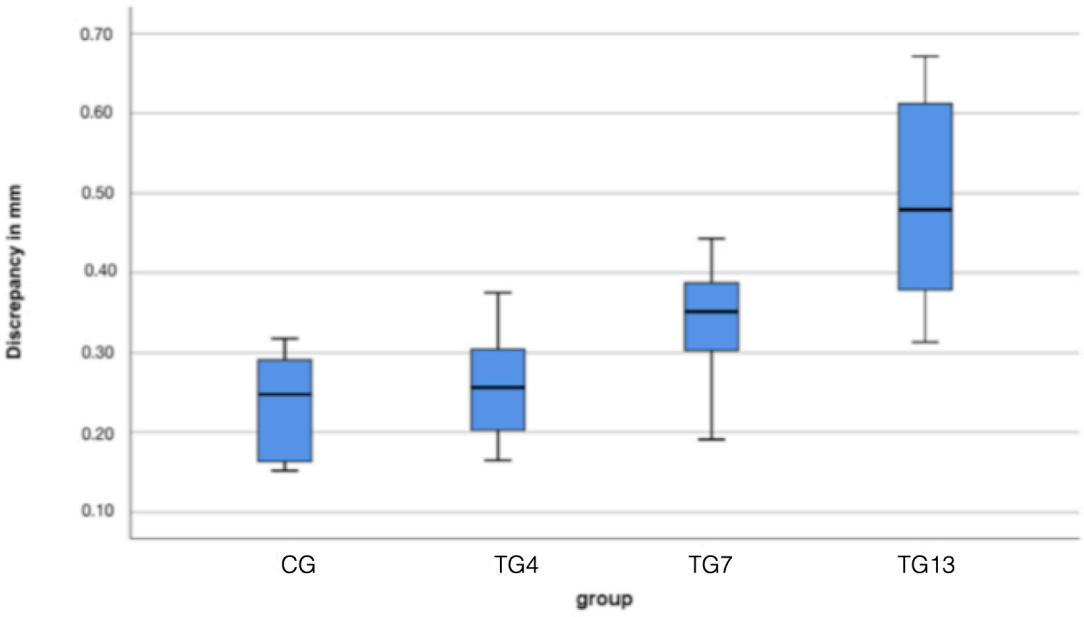

Figure 7: Side-by-side boxplots of the four groups, showing discrepancy in the horizontal plane in millimeters.

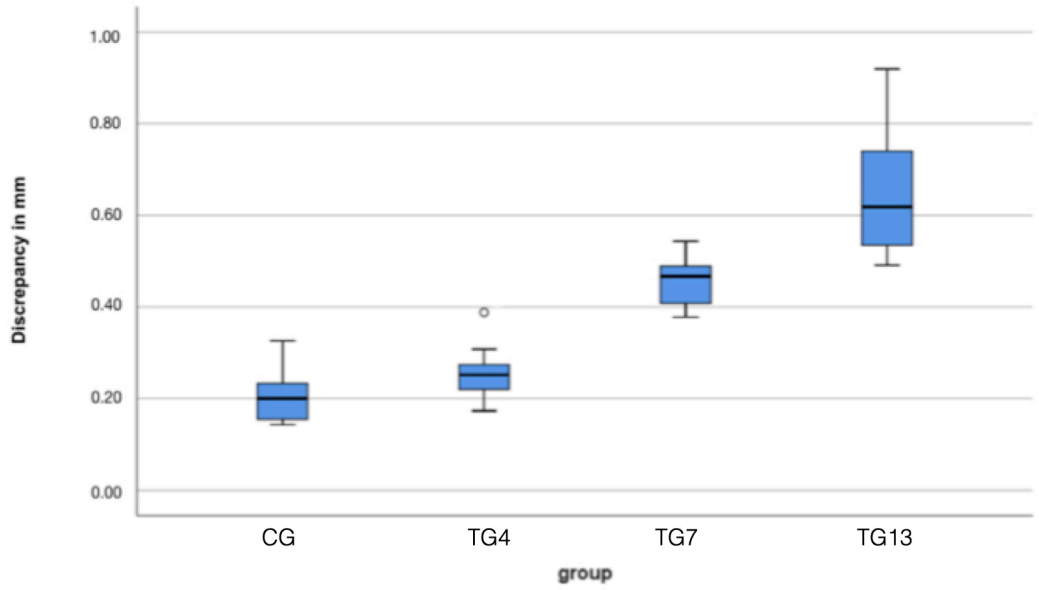

Figure 8: Side-by-side boxplots of the four groups, showing discrepancy in all three planes in millimeters.